taneous remyelination following extensive demyelination is associated with improved neurological function in a viral model of multiple sclerosis. Brain 124:1403–1416. CrossRef Medline

Oudega M, Varon S, Hagg T (1994) Regeneration of adult rat sensory axons into intraspinal nerve grafts: promoting effects of conditioning lesion and graft predegeneration. Exp Neurol 129:194–206. CrossRef Medline

Papastefanaki F, Chen J, Lavdas AA, Thomaidou D, Schachner M, Matsas R (2007) Grafts of Schwann cells engineered to express PSA-NCAM promote functional recovery after spinal cord injury. Brain 130:2159–2174. CrossRef Medline

Patel V, Joseph G, Patel A, Patel S, Bustin D, Mawson D, Tuesta LM, Puentes R, Ghosh M, Pearse DD (2010) Suspension matrices for improved Schwann-cell survival after implantation into the injured rat spinal cord. J Neurotrauma 27:789–801. CrossRef Medline

Paxinos G, Watson C (1998) The rat brain in stereotaxic coordinates, Ed 4. Sydney: Academic.

Pearse DD, Pereira FC, Marcillo AE, Bates ML, Berrocal YA, Filbin MT, Bunge MB (2004) cAMP and Schwann cells promote axonal growth and functional recovery after spinal cord injury. Nat Med 10:610–616. CrossRef Medline

Pearse DD, Sanchez AR, Pereira FC, Andrade CM, Puzis R, Pressman Y, Golden K, Kitay BM, Blits B, Wood PM, Bunge MB (2007) Transplantation of Schwann cells and/or olfactory ensheathing glia into the contused spinal cord: Survival, migration, axon association, and functional recovery. Glia 55:976–1000. CrossRef Medline

Petryniak MA, Potter GB, Rowitch DH, Rubenstein JL (2007) Dlx1 and Dlx2 control neuronal versus oligodendroglial cell fate acquisition in the developing forebrain. Neuron 55:417–433. CrossRef Medline

Plant GW, Bates ML, Bunge MB (2001) Inhibitory proteoglycan immunoreactivity is higher at the caudal than the rostral Schwann cell graft-transected spinal cord interface. Mol Cell Neurosci 17:471–487. CrossRef Medline

Rutkowski JL, Kirk CJ, Lerner MA, Tennekoon GI (1995) Purification and expansion of human Schwann cells in vitro. Nat Med 1:80–83. CrossRef Medline

Schwab ME, Bartholdi D (1996) Degeneration and regeneration of axons in the lesioned spinal cord. Physiol Rev 76:319–370. Medline

Shen Y, Tenney AP, Busch SA, Horn KP, Cuascut FX, Liu K, He Z, Silver J, Flanagan JG (2009) PTPsigma is a receptor for chondroitin sulfate proteoglycan, an inhibitor of neural regeneration. Science 326:592–596. CrossRef Medline

Silver J, Miller JH (2004) Regeneration beyond the glial scar. Nat Rev Neurosci 5:146–156. CrossRef Medline

Steward O, Zheng B, Tessier-Lavigne M (2003) False resurrections: distinguishing regenerated from spared axons in the injured central nervous system. J Comp Neurol 459:1–8. CrossRef Medline

Takami T, Oudega M, Bates ML, Wood PM, Kleitman N, Bunge MB (2002) Schwann cell but not olfactory ensheathing glia transplants improve hindlimb locomotor performance in the moderately contused adult rat thoracic spinal cord. J Neurosci 22:6670–6681. Medline

Tang X, Davies JE, Davies SJ (2003) Changes in distribution, cell associations, and protein expression levels of NG2, neurocan, phosphacan, brevican, versican V2, and tenascin-C during acute to chronic maturation of spinal cord scar tissue. J Neurosci Res 71:427–444. CrossRef Medline

Taylor L, Jones L, Tuszynski MH, Blesch A (2006) Neurotrophin-3 gradients established by lentiviral gene delivery promote short-distance axonal bridging beyond cellular grafts in the injured spinal cord. J Neurosci 26:9713–9721. CrossRef Medline

Tetzlaff W, Okon EB, Karimi-Abdolrezaee S, Hill CE, Sparling JS, Plemel JR, Plunet WT, Tsai EC, Baptiste D, Smithson LJ, Kawaja MD, Fehlings MG, Kwon BK (2011) A systematic review of cellular transplantation therapies for spinal cord injury. J Neurotrauma 28:1611–1682. CrossRef Medline

Urfer R, Tsoulfas P, Soppet D, Escandón E, Parada LF, Presta LG (1994) The binding epitopes of neurotrophin-3 to its receptors trkC and gp75 and the design of a multifunctional human neurotrophin. EMBO J 13:5896–5909. Medline

Vrinten DH, Hamers FF (2003) 'CatWalk' automated quantitative gait analysis as a novel method to assess mechanical allodynia in the rat; a comparison with von Frey testing. Pain 102:203–209. CrossRef Medline

Williams RR, Bunge MB (2012) Schwann cell transplantation: A repair strategy for spinal cord injury? Prog Brain Res 201:295–312.

Williams RR, Henao M, Pearse DD, Bunge MB (2013) Permissive Schwann cell graft/spinal cord interfaces for axon regeneration. Cell Transplant. Advance online publication. Retrieved Jan. 6, 2014. CrossRef Medline

Xu XM, Guénard V, Kleitman N, Bunge MB (1995) Axonal regeneration into Schwann cell-seeded guidance channels grafted into transected adult rat spinal cord. J Comp Neurol 351:145–160. CrossRef Medline

Xu XM, Chen A, Guénard V, Kleitman N, Bunge MB (1997) Bridging Schwann cell transplants promote axonal regeneration from both the rostral and caudal stumps of transected adult rat spinal cord. J Neurocytol 26:1–16. CrossRef Medline

Xu XM, Zhang SX, Li H, Aebischer P, Bunge MB (1999) Regrowth of axons into the distal spinal cord through a Schwann-cell-seeded mini-channel implanted into hemisected adult rat spinal cord. Eur J Neurosci 11:1723–1740. CrossRef Medline

Ying Z, Roy RR, Edgerton VR, Gómez-Pinilla F (2003) Voluntary exercise increases neurotrophin-3 and its receptor TrkC in the spinal cord. Brain Res 987:93–99. CrossRef Medline

Zhao RR, Muir EM, Alves JN, Rickman H, Allan AY, Kwok JC, Roet KC, Verhaagen J, Schneider BL, Bensadoun JC, Ahmed SG, Yáñez-Muñoz RJ, Keynes RJ, Fawcett JW, Rogers JH (2011) Lentiviral vectors express chondroitinase ABC in cortical projections and promote sprouting of injured corticospinal axons. J Neurosci Methods 201:228–238. CrossRef Medline

J Neurosurg 121:1514–1525, 2014

Low-energy extracorporeal shock wave therapy promotes vascular endothelial growth factor expression and improves locomotor recovery after spinal cord injury

Laboratory investigation

Seiji Yamaya, M.D.,[1] Hiroshi Ozawa, M.D., Ph.D.,[1] Haruo Kanno, M.D., Ph.D.,[1] Koshi N. Kishimoto, M.D., Ph.D.,[1] Akira Sekiguchi, M.D., Ph.D.,[1] Satoshi Tateda, M.D.,[1] Kenichiro Yahata, M.D.,[1] Kenta Ito, M.D., Ph.D.,[2] Hiroaki Shimokawa, M.D., Ph.D.,[2] and Eiji Itoi, M.D., Ph.D.[1]

Departments of [1]Orthopaedic Surgery and [2]Cardiovascular Medicine, Tohoku University Graduate School of Medicine, Sendai, Japan

Object. Extracorporeal shock wave therapy (ESWT) is widely used for the clinical treatment of various human diseases. Recent studies have demonstrated that low-energy ESWT upregulates the expression of vascular endothelial growth factor (VEGF) and promotes angiogenesis and functional recovery in myocardial infarction and peripheral artery disease. Many previous reports suggested that VEGF produces a neuroprotective effect to reduce secondary neural tissue damage after spinal cord injury (SCI). The purpose of the present study was to investigate whether low-energy ESWT promotes VEGF expression and neuroprotection and improves locomotor recovery after SCI.

Methods. Sixty adult female Sprague-Dawley rats were randomly divided into 4 groups: sham group (laminectomy only), sham-SW group (low-energy ESWT applied after laminectomy), SCI group (SCI only), and SCI-SW group (low-energy ESWT applied after SCI). Thoracic spinal cord contusion injury was inflicted using an impactor. Low-energy ESWT was applied to the injured spinal cord 3 times a week for 3 weeks. Locomotor function was evaluated using the Basso, Beattie, and Bresnahan (BBB) Scale (open field locomotor score) at different time points over 42 days after SCI. Hematoxylin and eosin staining was performed to assess neural tissue damage in the spinal cord. Neuronal loss was investigated by immunostaining for NeuN. The mRNA expressions of VEGF and its receptor, Flt-1, in the spinal cord were assessed using real-time polymerase chain reaction. Immunostaining for VEGF was performed to evaluate VEGF protein expression in the spinal cord.

Results. In both the sham and sham-SW groups, no animals showed locomotor impairment on BBB scoring. Histological analysis of H & E and NeuN stainings in the sham-SW group confirmed that no neural tissue damage was induced by the low-energy ESWT. Importantly, animals in the SCI-SW group demonstrated significantly better locomotor improvement than those in the SCI group at 7, 35, and 42 days after injury ($p < 0.05$). The number of NeuN-positive cells in the SCI-SW group was significantly higher than that in the SCI group at 42 days after injury ($p < 0.05$). In addition, mRNA expressions of VEGF and Flt-1 were significantly increased in the SCI-SW group compared with the SCI group at 7 days after injury ($p < 0.05$). The expression of VEGF protein in the SCI-SW group was significantly higher than that in the SCI group at 7 days ($p < 0.01$).

Conclusions. The present study showed that low-energy ESWT significantly increased expressions of VEGF and Flt-1 in the spinal cord without any detrimental effect. Furthermore, it significantly reduced neuronal loss in damaged neural tissue and improved locomotor function after SCI. These results suggested that low-energy ESWT enhances the neuroprotective effect of VEGF in reducing secondary injury and leads to better locomotor recovery following SCI. This study provides the first evidence that low-energy ESWT can be a safe and promising therapeutic strategy for SCI.
(http://thejns.org/doi/abs/10.3171/2014.8.JNS132562)

Key Words • **spinal cord injury** • **shock wave** • **VEGF** • **Flt-1** • **neuroprotection**

Abbreviations used in this paper: BBB = Basso, Beattie, Bresnahan; ESWT = extracorporeal shock wave therapy; HUVEC = human umbilical vein endothelial cell; NO = nitric oxide; PBS = phosphate-buffered saline; RT-PCR = real-time polymerase chain reaction; SCI = spinal cord injury; VEGF = vascular endothelial growth factor.

Extracorporeal shock wave therapy (ESWT) is widely used for the clinical treatment of various human diseases.[1,7,41–43] We have recently demonstrated that this therapy upregulates the expression of vascular endothelial growth factor (VEGF) in cultured

human umbilical vein endothelial cells (HUVECs) in vitro.[37] In addition, low-energy ESWT increases VEGF expression in ischemic tissues in vivo and promotes angiogenesis and functional recovery in models of chronic myocardial ischemia, myocardial infarction, and peripheral artery disease.[15,22–24,28,37,39,49,54] Moreover, it promotes neovascularization at the tendon-bone junction by increasing VEGF expression.[57]

Vascular endothelial growth factor is known as a stimulator of angiogenesis and a mediator of vascular permeability.[10,12,31,48] Previous studies showed that VEGF can stimulate both endothelial cells and neural cells and can provide neurotrophic, neuroprotective, and neuroproliferative effects.[11,17,40,52] It also suppresses the apoptosis of neuronal cultures, and the blockade of endogenous VEGF signaling increases cell death.[38]

Previous studies have demonstrated the therapeutic potential of VEGF in spinal cord injury (SCI).[11,32,53,60] The administration of a transcription factor engineered to increase VEGF expression suppresses axonal degeneration and apoptosis and promotes vascularity in a model of SCI.[32] In addition, the administration of recombinant VEGF increases the amount of spared tissue and blood vessels and reduces cell death and locomotor impairment after SCI.[60] On the other hand, the endogenous expression of VEGF in the injured spinal cord significantly decreases after SCI.[21] The decreased endogenous VEGF expression can worsen the pathophysiological process in SCI.[21]

If endogenous VEGF expression in the injured spinal cord can be upregulated by a noninvasive procedure, such as low-energy ESWT, it would be very useful for the clinical treatment of SCI. We hypothesized that low-energy ESWT would increase VEGF expression to induce neuroprotective effects and enhance locomotor recovery after SCI. In the present study, low-energy ESWT was applied to a spinal cord contusion model in rats to investigate VEGF expression and its therapeutic effect on SCI.

Methods

Animals

All experimental procedures were approved by the Institutional Animal Care and Use Committee of Tohoku University. All efforts were made to minimize both the number of animals used and the suffering of the animals. Sixty adult female Sprague-Dawley rats (body weight: 250–300 g) were used in the study (CLEA Japan). Six rats were included in each experimental group to evaluate locomotor function, as well as the histological analysis of neural tissue damage via H & E staining. Three rats per group were used to assess neuronal loss by counting the NeuN-stained cells. Four rats in each group at each time point were used to obtain real-time polymerase chain reaction (RT-PCR) results on VEGF and Flt-1 expression. Four rats per group were used for VEGF staining. The rats were housed 3–4 per cage and kept at a temperature of 24°C with free access to water and food before and after surgery.

The rats were randomly divided into the following 4 groups: sham group (laminectomy only), sham-SW group (low-energy ESWT applied after laminectomy), SCI group (SCI only), and SCI-SW group (low-energy ESWT applied after SCI). Random group allocation was performed to prevent bias in the study.

Spinal Cord Contusion Injury

The rats were anesthetized with 1.25% halothane in an oxygen/nitrous oxide (30/70%) gas mixture. During surgery, rectal temperature was monitored and maintained at 37.0 ± 0.5°C using a heating pad (Fine Science Tools Inc.). The skin above the vertebral column was shaved and cleaned with antiseptic. A midline skin incision was made, and the laminae of the T8–12 vertebrae were exposed. The T9–11 vertebrae were laminectomized to expose the dorsal cord surface with the dura mater intact. The vertebral column was stabilized with angled clamps attached to the T-8 and T-12 transverse processes. An SCI was induced with a New York University impactor (W.M. Keck Center for Collaborative Neuroscience).[5,18] A 10-g rod was dropped from 12.5 mm onto the T-10 segment. The impact rod was removed immediately after injury. The muscles and skin were closed in layers. To provide a reference marker for the application of the shock waves, a stitch of nylon thread was placed in the skin at the paravertebral muscle just above the injured spinal cord at T-10. Bladders were expressed twice a day until spontaneous voiding began. The sham-operated animals underwent the same surgical procedures, but no impact injury was inflicted.

Low-Energy ESWT

Low-energy ESWT was performed using a commercially available shock wave generator (DUOLITH-SD1, Storz Medical AG; Fig. 1A). Based on our previous studies,[15,20,22–24,28,37,39,49,50,54] the shock wave was applied to two spots on the injured spinal cord 3 times a week for 3 weeks after SCI. The treatment was performed immediately after wound closure following SCI, as well as 2, 4, 7, 9, 11, 14, 16, and 18 days after injury. Animals were anesthetized during each 5-minute treatment, as described above. The shock waves were 0.1 mJ/mm^2, 4 Hz, 200 shots/spot, with two spots for each treatment, as described previously.[15,22,28,37,39] According to the manufacturer's protocol, the optimal focal point of the shock wave is within a 10-mm width and a 10-mm depth from the tip of the probe (Fig. 1B), and 0.1 mJ/mm^2 (positive energy flux density) is equivalent to 0.25 mJ/mm^2 (total energy flux density). The focal point region was large enough to include the lesion of the spinal cord.

Behavioral Analysis

Locomotor function was evaluated using the Basso, Beattie, and Bresnahan (BBB) Scale (open field locomotor score) for 6 weeks after SCI.[5] The BBB Scale (from 0 to 21 points) can be used to assess locomotor recovery, including joint movements, stepping ability, coordination, and trunk stability. A score of 21 indicates unimpaired locomotion, as observed in uninjured rats. We also analyzed the BBB subscore (from 0 to 13 points), because some animals can show improvements in specific aspects

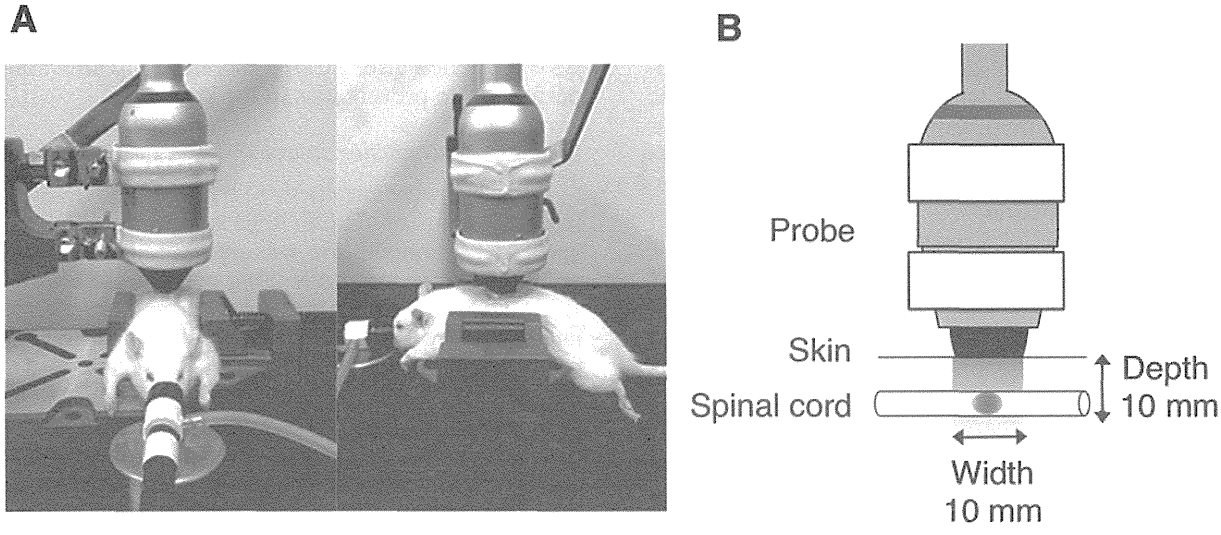

FIG. 1. Application of low-energy ESWT for SCI. **A:** Photographs showing that the shock wave probe was placed on the skin just behind the injured spinal cord between the T-8 and T-12 spinous processes. **B:** Illustration showing the optimal focal point of the shock wave was within a 10-mm width and a 10-mm depth from the tip of the probe.

of locomotion that do not follow a typical pattern of recovery and thus are not reflected in any change in the overall BBB score.[4] For these evaluations, the rats were individually placed in an open field with a nonslippery surface for 4 minutes, and in a blinded manner well-trained investigators rated them using the BBB Scale. Before surgery, the rats were individually placed in the open field for 4 minutes to ensure that all subjects consistently attained the maximum score. The BBB scores were measured at 4 and 24 hours and 7, 14, 21, 28, 35, and 42 days after SCI. An examiner blinded to rat group allocations performed all locomotor assessments.

Tissue Preparation

Seven and 42 days after SCI, the rats (8 and 36 rats, respectively) were overdosed with an intraperitoneal injection of 100 mg/kg of sodium pentobarbital. They were transcardially perfused with normal saline, followed by 4% paraformaldehyde in 0.1 M of phosphate-buffered saline (PBS) at pH 7.4. Spinal cord segments containing the injured site were collected, postfixed in the same fixative overnight at 4°C, and embedded in paraffin. Serial 7-μm transverse sections around the injured site were mounted on slides. Twenty-nine sequential sections at 250-μm intervals were collected from each rat, spanning a 7000-μm length in the spinal cord centered at the lesion epicenter. The serial sections were used for histological analyses as described below.

Hematoxylin and Eosin Staining

Serial transverse sections at 250-μm intervals around the lesion epicenter at 7 and 42 days after SCI were stained with H & E. Images of the stained sections were captured using a microscope (BX51, Olympus). For the other histological analyses, the tissue section with the least H & E–stained area was defined as the lesion epicenter for each animal.

To determine whether low-energy ESWT induces detrimental effects on the uninjured spinal cord, we assessed tissue damage in the spinal cord in the sham and sham-SW groups at 7 and 42 days. Given data from a previous study, we, in the present study, investigated the histological findings of tissue damage, such as hemorrhage, vacuole formation, and spindle-shaped changes of neurons in the spinal cord.[25,27,36] Histological analysis was performed using the H & E–stained serial transverse sections including the lesion epicenter. We determined whether the histological findings were present in both the white matter and the gray matter in each section by using microscopy. A pathologist confirmed the histological findings.

Immunohistochemistry

Immunohistochemical staining for NeuN was performed using the tissue sections obtained 42 days after SCI. In addition, the sections collected at 7 days after SCI were stained for VEGF. The sections were deparaffinized and rehydrated and then washed in PBS for 10 minutes, followed by washing with PBS containing 0.3% Tween for 10 minutes and blocking with 3% milk and 5% fetal bovine serum in 0.01 M of PBS for 2 hours. Tissue sections were incubated with a mouse anti-NeuN antibody (1:100, MAB377, Merck Millipore) or rabbit anti-VEGF antibody (1:50, sc-152, Santa Cruz Biotechnology) diluted in PBS overnight at 4°C. After rinsing with PBS, the sections were incubated with goat anti–mouse IgG Alexa Fluor 488 secondary antibody (1:500, Molecular Probes) or goat anti–rabbit IgG Alexa Fluor 594 secondary antibody (1:500, Molecular Probes) for 1 hour at room temperature. The sections were mounted on slides with Vectashield containing DAPI to label the nuclei (Vector Laboratories). In each experiment, all of the sections were stained at the same time.

Counting NeuN-Positive Cells

To investigate neuronal loss in the spinal cord, the

number of NeuN-positive cells in the sections was counted. After immunohistochemical staining of NeuN using the spinal cord sections from 42 days after SCI, as described above, each section was scanned using a microscope (BX51). The section at the 1500-μm-rostral, 1000-μm-rostral, 1000-μm-caudal, and 1500-μm-caudal area of the lesion epicenter was chosen for each animal. The scanned image of the transverse section was displayed on a monitor with a grid using the Photoshop Elements software program version 8.0 (Adobe Systems). All of the NeuN-positive cells in each grid were counted using a manual counter and then were added to obtain the total number of positive cells in the entire section. The NeuN-positive cells were defined as cells double-labeled with NeuN and DAPI. The number of NeuN-positive cells in the entire section at the areas 1500 μm rostral, 1000 μm rostral, 1000 μm caudal, and 1500 μm caudal to the lesion epicenter were counted and then compared among the groups at each location. The number of NeuN-positive cells was compared between the sham and sham-SW groups to investigate neuronal cell loss in the uninjured spinal cord after the application of low-energy ESWT. To evaluate the effects of low-energy ESWT after SCI, the number of NeuN-positive cells was also compared between the SCI and SCI-SW groups.

Quantitative RT-PCR

The spinal cord segments (10 mm in length) centered at the injury site were collected and harvested aseptically at 7 and 21 days after SCI and then were homogenized using a POLYTRON unit (Kinematica). Total RNA from the spinal cord was extracted using the TRIZOL reagent (Invitrogen) and cleaned up using a RNeasy Mini Kit (Qiagen) according to the manufacturer's protocol. First-strand cDNA synthesis and quantitative RT-PCR assays were performed to assess the mRNA expression levels of VEGF and its receptor, Flt-1. First-strand cDNA was synthesized using a high-capacity cDNA archive kit (Applied Biosystems). Quantitative RT-PCR was performed using ABI StepOnePlus, Power SYBR Green PCR MasterMix (Applied Biosystems), and 500 nM of each primer. These reactions were routinely run in duplicate. The primers were designed based on sequences in the GenBank database (F: 5′-GAGTTAAACGAACGTACTTGCAGA-3′ and R: 5′-TCTAGTTCCCGAAACCCTGA-3′ for VEGF, F: 5′-CAGTTTCCAAGTGGCCAGAG-3′ and R: 5′-AG GTCGCGATGAATGCAC-3′ for Flt-1, and F: 5′-CCCGC GAGTACAACCTTCT-3′ and R: 5′-CGTCATCCATG GCGAACT-3′ for β-actin). The fractional cycle number at which the fluorescence passes the threshold (Ct values) was used for quantification by using a comparative Ct method. The quantitated Ct values were obtained using the StepOne software program (version 2.1, Applied Biosystems). The Ct values of the gene of interest (Ct[GOI]) were standardized to those of β-actin (Ct[β-actin]). The results are shown as the $-\Delta Ct = -(Ct[GOI] - Ct[\beta\text{-actin}])$.[29]

Immunodensity Analysis of VEGF Staining

To evaluate VEGF protein expression in the injured spinal cord, we quantified the immunodensity of VEGF antibody staining in the spinal cord sections at 7 days after injury.[26] We photographed the entire transverse section at ×10 using a laser microscope with an image-capturing software program (BX51). The section 1500 μm rostral, 1000 μm rostral, 1000 μm caudal, and 1500 μm caudal to the lesion epicenter and the epicenter were chosen for each animal. For imaging, we determined in the first microscopy session the appropriate setting to avoid signal saturation and then used that same setting thereafter.

Using the ImageJ analysis system, we traced the whole spinal cord containing the lesion and perilesional areas in each section. Furthermore, we performed automatic thresholding for each image using the ImageJ software program to determine the threshold for a specific signal. The default threshold setting was used, and the thresholding values were maintained at constant levels for all analyses. After setting the threshold, the immunodensity above the threshold was automatically calculated.[26]

Statistical Analysis

A repeated-measures ANOVA with a Bonferroni post-hoc test was used to analyze differences in functional recovery between animal groups from 1 to 6 weeks postinjury. The significance of differences in the quantitative RT-PCR, the number of NeuN-positive cells, and the immunodensity of VEGF staining were analyzed using the unpaired t-test. In all analyses, a p value < 0.05 was considered to be statistically significant. All statistical analyses were performed using the GraphPad Prism 5.0a software program (GraphPad Software Inc.).

Results

BBB Locomotor Scores

To evaluate the effect of low-energy ESWT on locomotor function, the BBB score and subscore were measured for 6 weeks. In the sham and sham-SW groups, none of the animals showed any locomotor impairment and had full marks for the BBB score and subscore over 6 weeks (Fig. 2A and B). The SCI-SW group had significant locomotor improvement compared with the SCI group at 7, 35, and 42 days ($p < 0.05$; Fig. 2C). At 42 days after injury, the BBB scores in the SCI-SW group were 14–18 (mean 17 ± 1.6). In contrast, the BBB scores in the SCI group were 12–14 (mean 13 ± 0.9). Except for 1 rat with a BBB score of 14, the other 5 rats in the SCI-SW group achieved consistent plantar stepping and consistent forelimb-hindlimb coordination during gait; the predominant paw position was parallel at the initial contact and lift off at 42 days after injury. On the other hand, 4 of 6 rats in the SCI group did not keep their paws parallel when stepping, and they showed occasional or frequent forelimb-hindlimb coordination. The BBB subscore was significantly higher in the SCI-SW group than in the SCI group at 14, 21, 28, 35, and 42 days after injury ($p < 0.01$; Fig. 2D).

Histological Findings in H & E–Stained Spinal Cord Sections

In the histological analysis using H & E staining, no tissue damage was observed in the spinal cord at 7 and

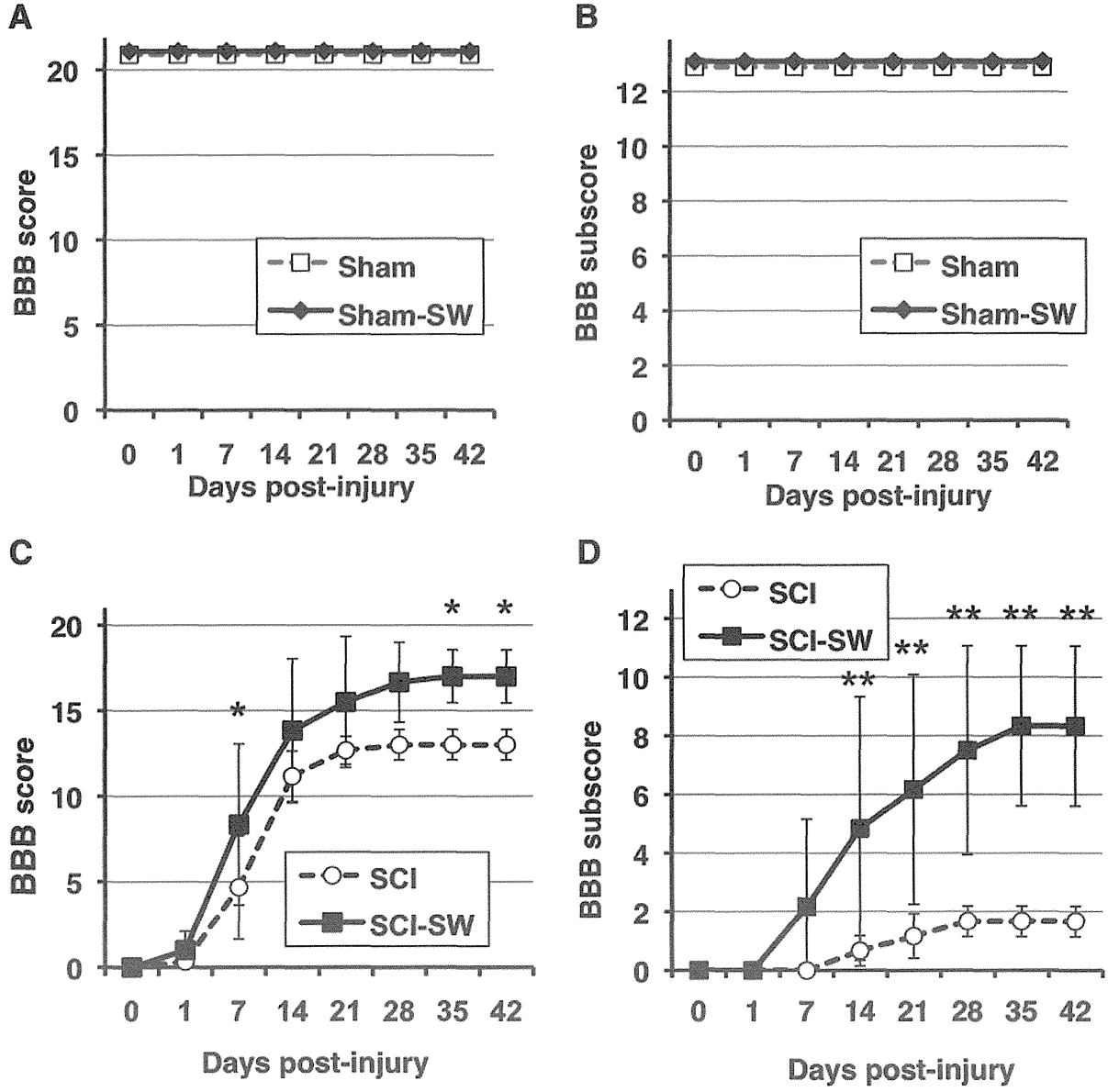

FIG. 2. **A and B:** In the sham and sham-SW groups, none of the animals showed any locomotor impairment and kept full marks for the BBB score and subscore over 6 weeks. **C:** The SCI-SW group demonstrated significantly better locomotor improvement, as reflected in BBB scoring, than did the SCI group at 7, 35, and 42 days after injury ($p < 0.05$). **D:** The BBB subscore was significantly higher in the SCI-SW group than in the SCI group at 14, 21, 28, 35, and 42 days ($p < 0.01$). Values represent the means ± standard deviation. *$p < 0.05$; **$p < 0.01$. Each group consisted of 6 animals.

42 days in either the sham or the sham-SW group (Fig. 3A–D). The low-energy ESWT caused no evident neural tissue damage, such as hemorrhage, vacuole formation, and spindle-shaped changes of neurons, in the uninjured spinal cord. Histological findings including hemorrhage and vacuole formation as well as cavity formation were observed in both the SCI and SCI-SW groups (Fig. 3E–H).

NeuN-Positive Cells

To investigate the loss of neuronal cells in the uninjured spinal cord after the application of low-energy ESWT, the number of NeuN-positive cells was compared between the sham and sham-SW groups at 42 days after sham injury. Representative NeuN-stained sections showed a similar number of NeuN-positive cells in the sham and sham-SW groups (Fig. 4A–L). There was no significant difference in the number of NeuN-positive cells between the sham and sham-SW groups (Fig. 4N).

To evaluate the neuroprotective effects of low-energy ESWT after SCI, the number of NeuN-positive cells was compared between the SCI and SCI-SW groups at 42 days after injury (Fig. 5A–L). In the SCI group, the NeuN-positive cells were sparsely observed at 1000 μm rostral to the lesion epicenter. In contrast, more NeuN-positive cells were observed in the SCI-SW group. The number of NeuN-positive cells in the SCI-SW group was

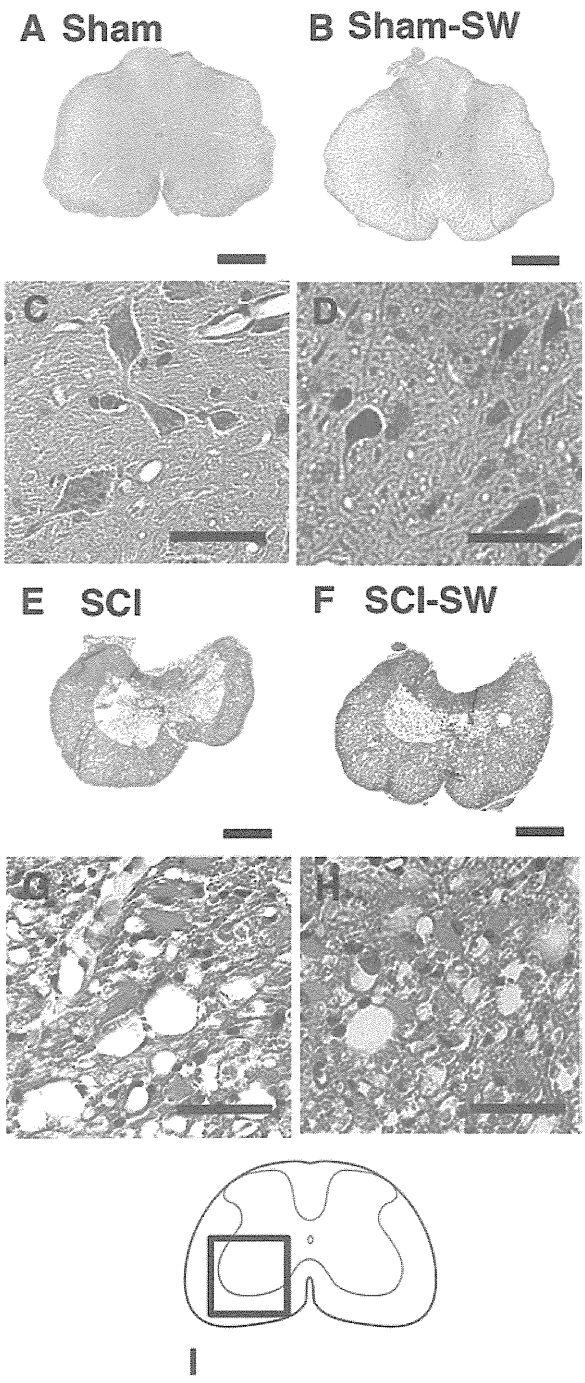

Fig. 3. Results of H & E staining performed to analyze neural tissue damage. **A and B:** In the sham and sham-SW groups, no tissue damage was observed in the spinal cord at 42 days (or 7 days, not shown). Bars = 500 μm. **C and D:** Magnified images showed no neural tissue damage, such as hemorrhage, spindle-shaped changes, or elongation of nuclei, in the spinal cord in either of these groups. Bars = 50 μm. **E and F:** Cavity formation was observed at the lesion epicenter in the SCI and SCI-SW groups. Bars = 500 μm. **G and H:** Magnified images showed the presence of neural tissue damage, such as hemorrhage and vacuole formation. Bars = 50 μm. **I:** Schematic illustrates the location of the micrographs. The histological analysis was performed using 6 animals per group.

significantly higher than that in the SCI group at 1000 μm rostral to the epicenter (313 ± 53.2 vs 78.3 ± 69.9, p = 0.010; Fig. 5N).

mRNA Expressions of VEGF and Flt-1

The mRNA expression levels of VEGF and Flt-1 were significantly higher in the SCI-SW group than in the SCI group at 7 days after injury (p = 0.018 and 0.004, respectively; Fig. 6). These mRNA expression levels in both the SCI and SCI-SW groups increased at 21 days, as compared with levels at 7 days. Expression levels of VEGF and Flt-1 were not significantly different between the groups at 21 days after SCI (p = 0.477 and 0.997, respectively).

Immunodensity of VEGF Staining

To investigate the protein expression of VEGF at 7 days after injury, the immunodensity of VEGF antibody staining was compared between the SCI and SCI-SW groups. The VEGF-positive cells were more frequently observed in the SCI-SW group than in the SCI group (Fig. 7A–L). The immunodensity of VEGF staining in the SCI-SW group was consistently higher than that in the SCI group from 1000 μm rostral to 1000 μm caudal to the lesion epicenter. Immunodensity at the epicenter was significantly different between the groups (p = 0.009; Fig. 7N).

Discussion

In the present study, low-energy ESWT induced no neural tissue damage in the spinal cord and produced no detrimental effect on locomotor function. In addition, it significantly increased the mRNA and protein expression levels of VEGF at 7 days after SCI. This treatment significantly reduced neuronal loss in the injured spinal cord. Furthermore, locomotor function was significantly improved in the animals treated with low-energy ESWT after SCI. These results demonstrated, for the first time, that low-energy ESWT promotes the neuroprotective effects of VEGF and leads to better locomotor recovery following SCI. Thus, low-energy ESWT has significant potential in the treatment of SCI.

The effects of the shock waves on tissues and organs is pressure dependent.[14] High-energy ESWT causes tissue injuries, such as microfracture and hematoma formation, in various tissues and organs.[19,42,45,55] It also causes injury to the neurovascular structures in the spinal cord and brain.[25,27,30] Histological findings of neural tissue damage, such as neuronal loss, contusional hemorrhage, and spindle-shaped changes in neurons, have been detected in the brain and spinal cord after the application of the high- or middle-energy shock waves.[27,30]

In contrast, low-energy ESWT induces no evident neural tissue damage in the spinal cord or brain. This is logical given that some researchers have suggested that the degree of neural tissue damage in the CNS caused by shock waves is pressure dependent.[27,30] In our study, low-energy ESWT caused no evident neural tissue damage, such as hemorrhage or spindle-shaped changes of neurons, in the uninjured spinal cord. In addition, NeuN

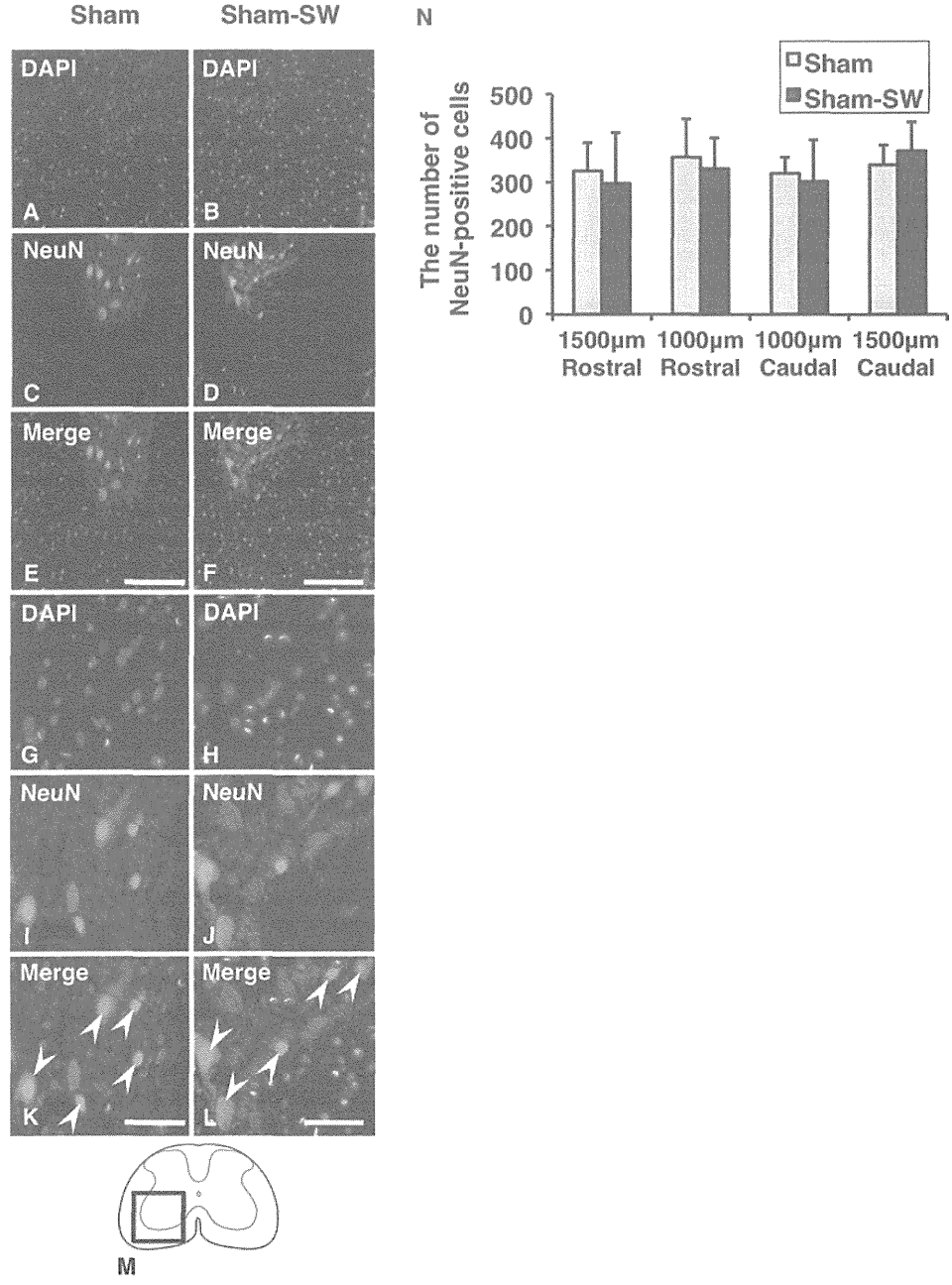

Fig. 4. Immunohistochemical staining of NeuN in the sham and sham-SW groups at 42 days after sham injury. **A–F:** Representative sections showed a similar number of NeuN-positive cells in the sham and sham-SW groups. Bars = 200 μm. **G–L:** Magnified images show NeuN-positive cells *(arrowheads)*. Bars = 50 μm. **M:** Schematic illustrates the location of the micrographs. **N:** The number of NeuN-positive cells was not significantly different between the sham and sham-SW groups. The histological analysis was performed using 3 animals per group. Values represent the means ± standard deviation.

staining revealed that no neuronal loss occurred in the uninjured spinal cord after the application of low-energy ESWT. Furthermore, locomotor function in sham-injured animals was not worsened by low-energy ESWT. These findings indicate that low-energy ESWT induces no detrimental effect on the spinal cord. Our study provides evidence to support the safety of low-energy ESWT for the treatment of SCI.

The application of shock waves can induce cavitation (a micrometer-sized violent collapse of bubbles) in the cells.[2] The physical force generated by cavitation produces localized shear stress on cell surface membranes.[13] The stress to the cells caused by the shock waves may lead to various biochemical effects.[9,16,34,35,47,51,58] We have previously shown that shock waves upregulate the expression of VEGF and its receptor, Flt-1, in various cells and organs.[37,39] Low-energy ESWT can upregulate the expression of both VEGF and Flt-1 in cultured HUVECs.[37] In

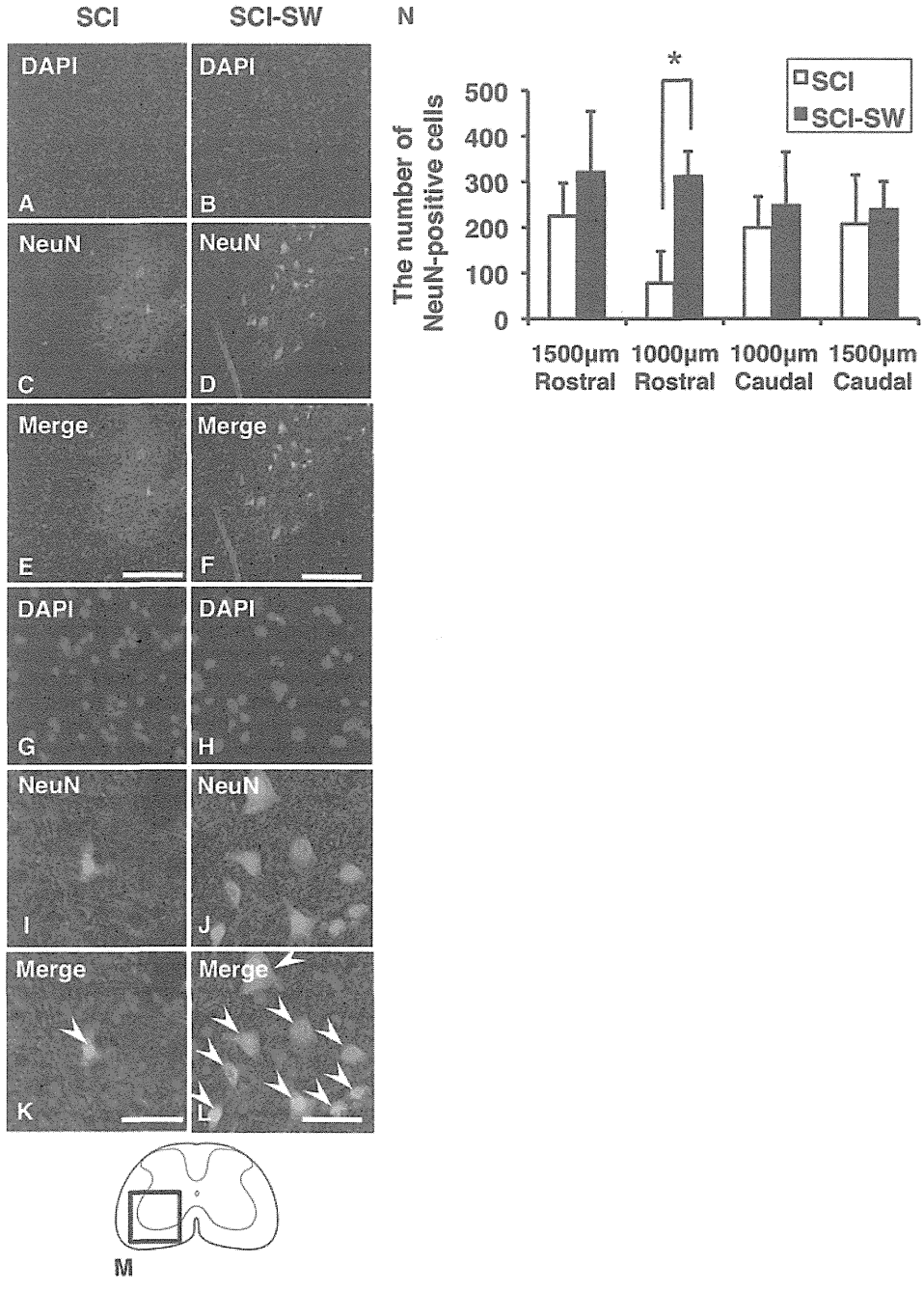

Fig. 5. Immunohistochemical staining of NeuN in the SCI and SCI-SW groups at 42 days after SCI. **A–F:** Representative sections at the position 1000 μm rostral from the lesion epicenter showed that there were more NeuN-positive cells in the SCI-SW than in the SCI group. Bars = 200 μm. **G–L:** Magnified images show the NeuN-positive cells *(arrowheads)*. The NeuN-positive cells were sparsely observed in the SCI group. Bars = 50 μm. **M:** Schematic illustrates the location of the micrographs. **N:** The number of NeuN-positive cells in the SCI-SW group was significantly higher than that in the SCI group at 1000 μm rostral from the epicenter ($p = 0.010$). The histological analysis was performed using 3 animals per group. Values represent the means ± standard deviation. *$p < 0.05$.

addition, low-energy ESWT increases the expression of VEGF in the ischemic tissues in chronic myocardial ischemia, acute myocardial infarction, and peripheral artery disease.[37,39] It has also enhanced lymphangiogenesis in a rat model of secondary lymphedema and accelerated skin wound healing in diabetic mice.[20,50] Data in the present study demonstrated that low-energy ESWT significantly upregulates mRNA expression levels of VEGF and Flt-1 in the spinal cord at 7 days after injury. Moreover, immunohistochemical analysis confirmed that there was a significant increase in the protein expression of VEGF in the injured spinal cord. These results indicate that low-energy ESWT can enhance the biological effects of VEGF in damaged neural tissue following SCI.

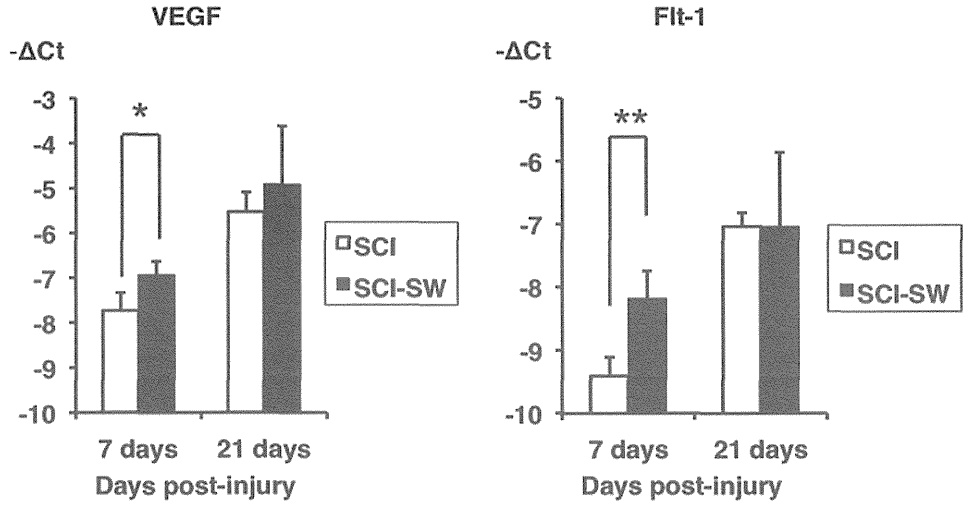

FIG. 6. The mRNA expression levels of VEGF and Flt-1 showed significant increases in the SCI-SW group compared with the SCI group at 7 days after SCI ($p = 0.018$ and 0.004, respectively). These mRNA expression levels in both groups were increased to the same or close to the same level at 21 days after the injury. This analysis was performed using 4 animals per group at each time point. $-\Delta Ct$ = a change in Ct values, which refers to the fractional cycle number at which the fluorescence passes the threshold. Values represent the means ± standard deviation. *$p < 0.05$; **$p < 0.01$.

In the developing nervous system, VEGF plays a pivotal role in vascularization and neuronal proliferation, as well as in the growth of coordinated vascular and neuronal networks. After injury to the nervous system, activation of VEGF and its receptors can restore the blood supply and promote neuronal survival and repair.[6] The upregulation of VEGF expression produces neuroprotective effects to reduce secondary injury and promotes vascularity as well as locomotor recovery after SCI.[32,60] Adenoviral VEGF administration promotes the regeneration of corticospinal tract axons in rats following transection of the spinal cord.[11] A previous report has suggested that the cytoprotective effects of VEGF are mediated through an antiapoptotic pathway.[62] Vascular endothelial growth factor stimulates nitric oxide (NO) release from the vascular endothelium and acts synergistically with NO to induce angiogenic and antiapoptotic effects.[33,44] Vascular endothelial growth factor can also perform multiple repair roles in the nervous system, including angiogenic, blood-brain barrier permeabilizing, and neurotrophic actions.[44,46] In the present study, expression levels of VEGF and Flt-1 in the injured spinal cord were significantly increased by the low-energy ESWT at 7 days after SCI. This treatment significantly reduced neuronal loss in the injured spinal cord and promoted locomotor recovery after SCI. Therefore, the increased expression of VEGF induced by the low-energy ESWT may provide neuroprotective effects that improve locomotor function after SCI.

Previous studies have demonstrated that the mRNA and protein expression levels of VEGF in the spinal cord are decreased in the acute and subacute phases (from 12 hours to 14 days) after SCI.[3,21,46,56] The decreased level of VEGF expression may cause a reduction in the endogenous neuroprotective function and worsen secondary damage after SCI.[21] Importantly, our results revealed that low-energy ESWT significantly upregulates VEGF and Flt-1 expression levels in the injured spinal cord at 7 days after injury. Previous studies have shown that the upregulation of VEGF expression starts to be seen within 7 days after the application of low-energy ESWT in various disease models.[51,57,61] These results suggest that the application of low-energy ESWT in the acute phase of SCI can reinforce the neuroprotective effect of VEGF and reduce the secondary damage following SCI.

The application of shock waves can regulate VEGF expression as well as induce various other biochemical effects, such as nonenzymatic NO synthesis, Ras activation, and expression of several chemokines and matrix metalloproteinases to provide anti-inflammatory effects.[9,34,35,51,58] A previous study showed that ESWT enhances endothelial NO synthase activity and intracellular NO production in HUVECs and produces an anti-inflammatory effect.[35] Extracorporeal shock wave therapy downregulates NF-κB activation and NF-κB–dependent gene expression, such as the expression of inducible NO synthase and tumor necrosis factor-α, and consequently induces an anti-inflammatory effect.[9] Additionally, ESWT can enhance the expression of growth factors, including BMP-2 and transforming growth factor-β, at treated sites.[8,59] Therefore, VEGF as well as other factors may induce a neuroprotective effect after the application of low-energy ESWT following SCI. It is unclear which type of cell in the spinal cord expresses VEGF in response to low-energy ESWT. The molecular mechanisms underlying the upregulation of VEGF expression induced by the low-energy ESWT needs to be elucidated in future studies. Further analysis of this therapy may lead to a detailed understanding of the molecular and biochemical mechanism and clinical application of this treatment for SCI. In the present study, the protocol used for ESWT application was based on those in previous studies, and only a single application of the shock waves was used. A different protocol for ESWT application may induce better effects on the injured spinal cord.

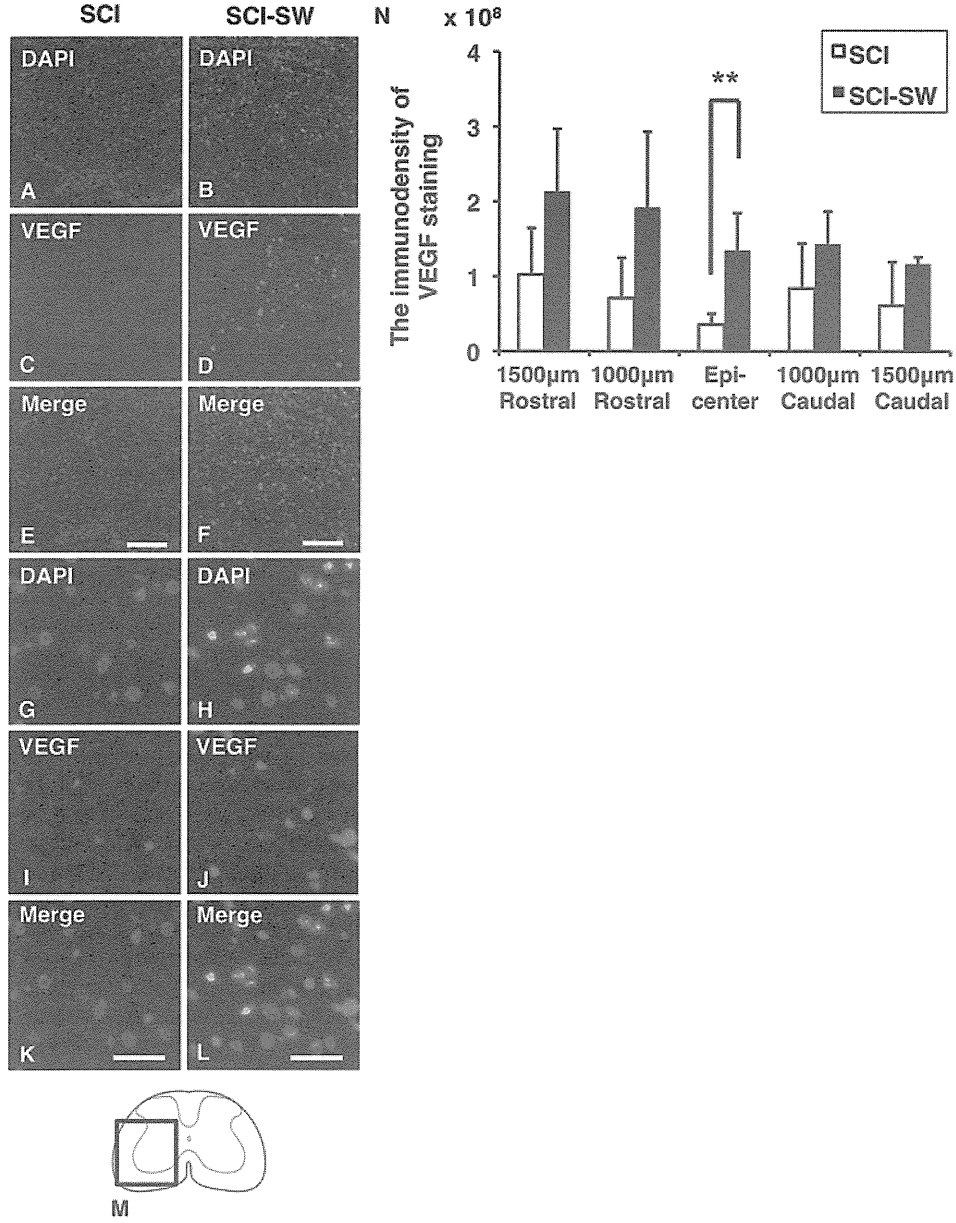

Fig. 7. Immunohistochemical staining of VEGF after SCI. **A–F:** In representative spinal cord sections at the lesion epicenter, the VEGF-positive cells were more frequently observed in the SCI-SW group than in the SCI group. Bars = 100 μm. **G–L:** Magnified images show the VEGF-positive cells. Bars = 25 μm. **M:** Schematic illustrates the location of the micrographs. **N:** The immunodensity of VEGF staining at the lesion epicenter was significantly higher in the SCI-SW group than in the SCI group ($p = 0.009$). The histological analysis was performed using 4 animals per group. Values represent the means ± standard deviation. $^{**}p < 0.01$.

In the clinical treatment of SCI, low-energy ESWT would be applied to the spinal cord from the dorsal side of the patients. Because bone as well as metal can interfere with the effects of shock waves, this extracorporeal treatment is suitable for patients after decompression surgery, such as laminectomy, at the lesion site. In patients treated with spinal fixation, the instruments should not be located between the probe delivering the shock wave and the lesion site on the spinal cord. A major advantage of low-energy ESWT is that it is noninvasive and safe, without any adverse effects or procedural complications.[15,37,54] If necessary, patients with SCI can undergo low-energy ESWT repeatedly, and the procedure is easy to perform because it does not require the induction of anesthesia, catheter intervention, or drug administration.

Conclusions

Findings in the present study showed that low-energy ESWT significantly increases expressions of VEGF and Flt-1 in the spinal cord without any detrimental effect. Furthermore, low-energy ESWT significantly reduced neuronal loss in damaged neural tissue and improved lo-

comotor function after SCI. These results demonstrated that low-energy ESWT enhances the neuroprotective effect of VEGF and leads to better locomotor recovery following SCI. This study provides the first evidence that low-energy ESWT can be a safe and promising therapeutic strategy for SCI.

Acknowledgments

We thank Mr. Katsuyoshi Shoji for technical assistance and Ms. Teruko Sueta and the animal care team at the Institute for Animal Experimentation of Tohoku University for the animal care in this study.

Disclosure

The authors report no conflict of interest concerning the materials or methods used in this study or the findings specified in this paper. This work was supported by a Grant-in-Aid for Scientific Research (C) (No. 10312563) from the Japan Society for the Promotion of Science and by Grants-in-Aid from the Japanese Ministry of Health, Labor and Welfare, Tokyo, Japan (H21-rinsyokenkyu-ippan-012).

Author contributions to the study and manuscript preparation include the following. Conception and design: Kanno, Yamaya, Ozawa, Ito, Shimokawa, Itoi. Acquisition of data: Kanno, Yamaya. Analysis and interpretation of data: Kanno, Yamaya, Kishimoto. Drafting the article: Kanno, Yamaya. Critically revising the article: all authors. Reviewed submitted version of manuscript: all authors. Approved the final version of the manuscript on behalf of all authors: Kanno. Statistical analysis: Yamaya. Administrative/technical/material support: Kishimoto, Sekiguchi, Tateda, Yahata, Ito, Shimokawa. Study supervision: Kanno, Ozawa, Kishimoto, Ito, Shimokawa, Itoi.

References

1. Al-Abbad H, Simon JV: The effectiveness of extracorporeal shock wave therapy on chronic Achilles tendinopathy: a systematic review. **Foot Ankle Int 34:**33–41, 2013
2. Apfel RE: Acoustic cavitation: a possible consequence of biomedical uses of ultrasound. **Br J Cancer Suppl 5:**140–146, 1982
3. Bartholdi D, Rubin BP, Schwab ME: VEGF mRNA induction correlates with changes in the vascular architecture upon spinal cord damage in the rat. **Eur J Neurosci 9:**2549–2560, 1997
4. Basso DM: Behavioral testing after spinal cord injury: congruities, complexities, and controversies. **J Neurotrauma 21:** 395–404, 2004
5. Basso DM, Beattie MS, Bresnahan JC: A sensitive and reliable locomotor rating scale for open field testing in rats. **J Neurotrauma 12:**1–21, 1995
6. Brockington A, Lewis C, Wharton S, Shaw PJ: Vascular endothelial growth factor and the nervous system. **Neuropathol Appl Neurobiol 30:**427–446, 2004
7. Cacchio A, Giordano L, Colafarina O, Rompe JD, Tavernese E, Ioppolo F, et al: Extracorporeal shock-wave therapy compared with surgery for hypertrophic long-bone nonunions. **J Bone Joint Surg Am 91:**2589–2597, 2009
8. Chen YJ, Wurtz T, Wang CJ, Kuo YR, Yang KD, Huang HC, et al: Recruitment of mesenchymal stem cells and expression of TGF-beta 1 and VEGF in the early stage of shock wave-promoted bone regeneration of segmental defect in rats. **J Orthop Res 22:**526–534, 2004
9. Ciampa AR, de Prati AC, Amelio E, Cavalieri E, Persichini T, Colasanti M, et al: Nitric oxide mediates anti-inflammatory action of extracorporeal shock waves. **FEBS Lett 579:**6839–6845, 2005
10. Connolly DT, Olander JV, Heuvelman D, Nelson R, Monsell R, Siegel N, et al: Human vascular permeability factor. Isolation from U937 cells. **J Biol Chem 264:**20017–20024, 1989
11. Facchiano F, Fernandez E, Mancarella S, Maira G, Miscusi M, D'Arcangelo D, et al: Promotion of regeneration of corticospinal tract axons in rats with recombinant vascular endothelial growth factor alone and combined with adenovirus coding for this factor. **J Neurosurg 97:**161–168, 2002
12. Ferrara N, Gerber HP, LeCouter J: The biology of VEGF and its receptors. **Nat Med 9:**669–676, 2003
13. Fisher AB, Chien S, Barakat AI, Nerem RM: Endothelial cellular response to altered shear stress. **Am J Physiol Lung Cell Mol Physiol 281:**L529–L533, 2001
14. Fuchs GJ, David RD, Fuchs AM: [Complications of extracorporeal shockwave lithotripsy.] **Arch Esp Urol 42 (Suppl 1):**83–89, 1989 (Span)
15. Fukumoto Y, Ito A, Uwatoku T, Matoba T, Kishi T, Tanaka H, et al: Extracorporeal cardiac shock wave therapy ameliorates myocardial ischemia in patients with severe coronary artery disease. **Coron Artery Dis 17:**63–70, 2006
16. Gotte G, Amelio E, Russo S, Marlinghaus E, Musci G, Suzuki H: Short-time non-enzymatic nitric oxide synthesis from L-arginine and hydrogen peroxide induced by shock waves treatment. **FEBS Lett 520:**153–155, 2002
17. Greenberg DA, Jin K: From angiogenesis to neuropathology. **Nature 438:**954–959, 2005
18. Gruner JA: A monitored contusion model of spinal cord injury in the rat. **J Neurotrauma 9:**123–128, 1992
19. Haupt G: Use of extracorporeal shock waves in the treatment of pseudarthrosis, tendinopathy and other orthopedic diseases. **J Urol 158:**4–11, 1997
20. Hayashi D, Kawakami K, Ito K, Ishii K, Tanno H, Imai Y, et al: Low-energy extracorporeal shock wave therapy enhances skin wound healing in diabetic mice: a critical role of endothelial nitric oxide synthase. **Wound Repair Regen 20:**887–895, 2012
21. Herrera JJ, Nesic O, Narayana PA: Reduced vascular endothelial growth factor expression in contusive spinal cord injury. **J Neurotrauma 26:**995–1003, 2009
22. Ito K, Fukumoto Y, Shimokawa H: Extracorporeal shock wave therapy as a new and non-invasive angiogenic strategy. **Tohoku J Exp Med 219:**1–9, 2009
23. Ito K, Fukumoto Y, Shimokawa H: Extracorporeal shock wave therapy for ischemic cardiovascular disorders. **Am J Cardiovasc Drugs 11:**295–302, 2011
24. Ito Y, Ito K, Shiroto T, Tsuburaya R, Yi GJ, Takeda M, et al: Cardiac shock wave therapy ameliorates left ventricular remodeling after myocardial ischemia-reperfusion injury in pigs in vivo. **Coron Artery Dis 21:**304–311, 2010
25. Karatas A, Dosoglu M, Zeyrek T, Kayikci A, Erol A, Can B: The effect of extracorporeal shock wave lithotripsy on the rat spinal cord. **Spinal Cord 46:**627–632, 2008
26. Karimi-Abdolrezaee S, Eftekharpour E, Wang J, Schut D, Fehlings MG: Synergistic effects of transplanted adult neural stem/progenitor cells, chondroitinase, and growth factors promote functional repair and plasticity of the chronically injured spinal cord. **J Neurosci 30:**1657–1676, 2010
27. Kato K, Fujimura M, Nakagawa A, Saito A, Ohki T, Takayama K, et al: Pressure-dependent effect of shock waves on rat brain: induction of neuronal apoptosis mediated by a caspase-dependent pathway. **J Neurosurg 106:**667–676, 2007
28. Kikuchi Y, Ito K, Ito Y, Shiroto T, Tsuburaya R, Aizawa K, et al: Double-blind and placebo-controlled study of the effectiveness and safety of extracorporeal cardiac shock wave therapy for severe angina pectoris. **Circ J 74:**589–591, 2010
29. Kishimoto KN, Oxford CL, Reddi AH: Stimulation of the side population fraction of ATDC5 chondroprogenitors by hypoxia. **Cell Biol Int 33:**1222–1229, 2009
30. Lee TC, Huang HY, Yang YL, Hung KS, Cheng CH, Chang NK, et al: Vulnerability of the spinal cord to injury from ex-

tracorporeal shock waves in rabbits. **J Clin Neurosci 14:**873–878, 2007
31. Leung DW, Cachianes G, Kuang WJ, Goeddel DV, Ferrara N: Vascular endothelial growth factor is a secreted angiogenic mitogen. **Science 246:**1306–1309, 1989
32. Liu Y, Figley S, Spratt SK, Lee G, Ando D, Surosky R, et al: An engineered transcription factor which activates VEGF-A enhances recovery after spinal cord injury. **Neurobiol Dis 37:**384–393, 2010
33. Luo Z, Diaco M, Murohara T, Ferrara N, Isner JM, Symes JF: Vascular endothelial growth factor attenuates myocardial ischemia-reperfusion injury. **Ann Thorac Surg 64:**993–998, 1997
34. Mariotto S, Cavalieri E, Amelio E, Ciampa AR, de Prati AC, Marlinghaus E, et al: Extracorporeal shock waves: from lithotripsy to anti-inflammatory action by NO production. **Nitric Oxide 12:**89–96, 2005
35. Mariotto S, de Prati AC, Cavalieri E, Amelio E, Marlinghaus E, Suzuki H: Extracorporeal shock wave therapy in inflammatory diseases: molecular mechanism that triggers anti-inflammatory action. **Curr Med Chem 16:**2366–2372, 2009
36. Nakagawa A, Manley GT, Gean AD, Ohtani K, Armonda R, Tsukamoto A, et al: Mechanisms of primary blast-induced traumatic brain injury: insights from shock-wave research. **J Neurotrauma 28:**1101–1119, 2011
37. Nishida T, Shimokawa H, Oi K, Tatewaki H, Uwatoku T, Abe K, et al: Extracorporeal cardiac shock wave therapy markedly ameliorates ischemia-induced myocardial dysfunction in pigs in vivo. **Circulation 110:**3055–3061, 2004
38. Ogunshola OO, Antic A, Donoghue MJ, Fan SY, Kim H, Stewart WB, et al: Paracrine and autocrine functions of neuronal vascular endothelial growth factor (VEGF) in the central nervous system. **J Biol Chem 277:**11410–11415, 2002
39. Oi K, Fukumoto Y, Ito K, Uwatoku T, Abe K, Hizume T, et al: Extracorporeal shock wave therapy ameliorates hindlimb ischemia in rabbits. **Tohoku J Exp Med 214:**151–158, 2008
40. Oosthuyse B, Moons L, Storkebaum E, Beck H, Nuyens D, Brusselmans K, et al: Deletion of the hypoxia-response element in the vascular endothelial growth factor promoter causes motor neuron degeneration. **Nat Genet 28:**131–138, 2001
41. Pan PJ, Chou CL, Chiou HJ, Ma HL, Lee HC, Chan RC: Extracorporeal shock wave therapy for chronic calcific tendinitis of the shoulders: a functional and sonographic study. **Arch Phys Med Rehabil 84:**988–993, 2003
42. Rompe JD, Kirkpatrick CJ, Küllmer K, Schwitalle M, Krischek O: Dose-related effects of shock waves on rabbit tendo Achillis. A sonographic and histological study. **J Bone Joint Surg Br 80:**546–552, 1998
43. Rompe JD, Meurer A, Nafe B, Hofmann A, Gerdesmeyer L: Repetitive low-energy shock wave application without local anesthesia is more efficient than repetitive low-energy shock wave application with local anesthesia in the treatment of chronic plantar fasciitis. **J Orthop Res 23:**931–941, 2005
44. Rosenstein JM, Krum JM: New roles for VEGF in nervous tissue—beyond blood vessels. **Exp Neurol 187:**246–253, 2004
45. Salem S, Mehrsai A, Zartab H, Shahdadi N, Pourmand G: Complications and outcomes following extracorporeal shock wave lithotripsy: a prospective study of 3,241 patients. **Urol Res 38:**135–142, 2010
46. Savas S, Savas C, Altuntas I, Adiloglu A: The correlation between nitric oxide and vascular endothelial growth factor in spinal cord injury. **Spinal Cord 46:**113–117, 2008
47. Seidl M, Steinbach P, Wörle K, Hofstädter F: Induction of stress fibres and intercellular gaps in human vascular endothelium by shock-waves. **Ultrasonics 32:**397–400, 1994
48. Senger DR, Galli SJ, Dvorak AM, Perruzzi CA, Harvey VS, Dvorak HF: Tumor cells secrete a vascular permeability factor that promotes accumulation of ascites fluid. **Science 219:** 983–985, 1983
49. Serizawa F, Ito K, Kawamura K, Tsuchida K, Hamada Y, Zukeran T, et al: Extracorporeal shock wave therapy improves the walking ability of patients with peripheral artery disease and intermittent claudication. **Circ J 76:**1486–1493, 2012
50. Serizawa F, Ito K, Matsubara M, Sato A, Shimokawa H, Satomi S: Extracorporeal shock wave therapy induces therapeutic lymphangiogenesis in a rat model of secondary lymphoedema. **Eur J Vasc Endovasc Surg 42:**254–260, 2011
51. Stojadinovic A, Elster EA, Anam K, Tadaki D, Amare M, Zins S, et al: Angiogenic response to extracorporeal shock wave treatment in murine skin isografts. **Angiogenesis 11:**369–380, 2008
52. Svensson B, Peters M, König HG, Poppe M, Levkau B, Rothermundt M, et al: Vascular endothelial growth factor protects cultured rat hippocampal neurons against hypoxic injury via an antiexcitotoxic, caspase-independent mechanism. **J Cereb Blood Flow Metab 22:**1170–1175, 2002
53. Tator CH, Fehlings MG: Review of the secondary injury theory of acute spinal cord trauma with emphasis on vascular mechanisms. **J Neurosurg 75:**15–26, 1991
54. Uwatoku T, Ito K, Abe K, Oi K, Hizume T, Sunagawa K, et al: Extracorporeal cardiac shock wave therapy improves left ventricular remodeling after acute myocardial infarction in pigs. **Coron Artery Dis 18:**397–404, 2007
55. Valchanou VD, Michailov P: High energy shock waves in the treatment of delayed and nonunion of fractures. **Int Orthop 15:**181–184, 1991
56. Vaquero J, Zurita M, de Oya S, Coca S: Vascular endothelial growth/permeability factor in spinal cord injury. **J Neurosurg 90 (2 Suppl):**220–223, 1999
57. Wang CJ, Wang FS, Yang KD, Weng LH, Hsu CC, Huang CS, et al: Shock wave therapy induces neovascularization at the tendon-bone junction. A study in rabbits. **J Orthop Res 21:** 984–989, 2003
58. Wang FS, Wang CJ, Huang HJ, Chung H, Chen RF, Yang KD: Physical shock wave mediates membrane hyperpolarization and Ras activation for osteogenesis in human bone marrow stromal cells. **Biochem Biophys Res Commun 287:**648–655, 2001
59. Wang FS, Yang KD, Kuo YR, Wang CJ, Sheen-Chen SM, Huang HC, et al: Temporal and spatial expression of bone morphogenetic proteins in extracorporeal shock wave-promoted healing of segmental defect. **Bone 32:**387–396, 2003
60. Widenfalk J, Lipson A, Jubran M, Hofstetter C, Ebendal T, Cao Y, et al: Vascular endothelial growth factor improves functional outcome and decreases secondary degeneration in experimental spinal cord contusion injury. **Neuroscience 120:**951–960, 2003
61. Yan X, Zeng B, Chai Y, Luo C, Li X: Improvement of blood flow, expression of nitric oxide, and vascular endothelial growth factor by low-energy shockwave therapy in random-pattern skin flap model. **Ann Plast Surg 61:**646–653, 2008
62. Zachary I: Neuroprotective role of vascular endothelial growth factor: signalling mechanisms, biological function, and therapeutic potential. **Neurosignals 14:**207–221, 2005

Manuscript submitted November 22, 2013.
Accepted August 18, 2014.
Portions of this work were presented as proceedings in abstract form at the Annual Meeting of American Academy of Orthopaedic Surgeons held in Chicago, Illinois, March 19–23, 2013.
Please include this information when citing this paper: published online October 3, 2014; DOI: 10.3171/2014.8.JNS132562.
Address correspondence to: Haruo Kanno, M.D., Ph.D., Department of Orthopaedic Surgery, Tohoku University Graduate School of Medicine, 1-1 Seiryo-machi, Aoba-ku, Sendai, Miyagi 980-8574, Japan. email: kanno-h@isis.ocn.ne.jp.

Chapter 29
Clinical Significance of 3D-MRI/^{18}F-FDG PET Fusion Imaging of Patients with Cervical Compressive Myelopathy

Kenzo Uchida, Hideaki Nakajima, Hidehiko Okazawa, Hirohiko Kimura, Ai Yoshida, and Hisatoshi Baba

Abstract The present study was designed to evaluate the use of three-dimensional (3D)-MRI/^{18}F-FDG PET fusion imaging to define intramedullary signal changes on MRIs and local glucose metabolic rate measured on ^{18}F-FDG PET in relation to clinical outcome and prognosis. Quantitative analysis of intramedullary signal changes on MRIs included calculation of the signal intensity ratio (SIR). On fusion images, the maximal count at the lesion was adopted as the standardized uptake value (SUV_{max}). The SUV ratio (SUVR) was also calculated. Neurological assessment was conducted using the Japanese Orthopaedic Association (JOA) scoring system. The SIR on T1-weighted images (WIs), but not SIR on T2-WIs, correlated with preoperative JOA score and postoperative neurological improvement. Lesion-SUVmax correlated with SIR on T1-WIs, but not with SIR on T2-WIs, and also with postoperative neurological outcome. The SUVR correlated better than SIR on T1-WIs and lesion-SUV_{max} with neurological improvement. Longer symptom duration correlated negatively with SIR on T1-WIs, positively with SIR on T2-WIs, and negatively with SUV_{max}. Our results suggest that low-intensity signal on the T1-WIs correlates with poor postoperative neurological outcome. SUV_{max} measured at lesions with increased signal intensity and SUVR measured on fusion MRI/PET are sensitive parameters for prediction of clinical outcome.

K. Uchida (✉) • H. Nakajima • H. Baba • A. Yoshida
Faculty of Medical Sciences, Department of Orthopaedics and Rehabilitation Medicine, University of Fukui, Matsuoka Shimoaizuki 23-3, Eiheiji, Fukui 910-1193, Japan
e-mail: kuchida@u-fukui.ac.jp

H. Okazawa
Biomedical Imaging Research Center, University of Fukui, Matsuoka Shimoaizuki 23, Eiheiji, Fukui 910-1193, Japan

H. Kimura
Department of Radiology, Faculty of Medical Sciences, University of Fukui, Matsuoka Shimoaizuki 23, Eiheiji, Fukui 910-1193, Japan

K. Uchida et al. (eds.), *Neuroprotection and Regeneration of the Spinal Cord*,
DOI 10.1007/978-4-431-54502-6_29, © Springer Japan 2014

Keywords [^{18}F]-fluorodeoxyglucose (FDG) positron emission tomography (PET) • Cervical myelopathy • Fusion imaging • MRI • Spinal cord

29.1 Introduction

It is important to assess spinal cord function in patients amenable to neurosurgical treatment for cervical compressive myelopathy. The majority of the conventional tests focus on evaluation of neural conductivity across the damaged spinal cord [1] or morphological and pathological changes at the compressed cord that can be identified on magnetic resonance imaging (MRI). MRI is a valuable tool before surgical decompression because it visualizes not only the magnitude of spinal cord compression but also the intramedullary signal intensity. Many authors have reported changes in intramedullary high-signal intensity on T2-weighted MR imaging in patients with compressive spondylotic lesions of the cervical spinal cord [2–5]. Such abnormality in intramedullary high-signal intensity is considered to represent myelomalacia or cord gliosis secondary to a long-standing compression of the spinal cord [4]. Therefore, the presence of intramedullary high-signal intensity in patients with compressive myelopathy indicates the existence of a chronic spinal cord compressive lesion. However, the prognostic capacity of these imaging parameters remains controversial, especially with regard to the change in signal intensity of the spinal cord on T2-weighted MRI. The cause of controversy is thought to be the lack of quantitative assessment of these changes in signal intensity.

[^{18}F]-fluorodeoxyglucose (FDG) positron emission tomography (PET) has been used to investigate neural tissue metabolic activity including that of the spinal cord [6]. We used high-resolution ^{18}F-FDG PET to visualize the cervical spinal cord and quantify its metabolic activity [7] and also reported that patients with cervical myelopathy have a variable degree of glucose utilization rate in the whole cervical spinal cord [8] and that impaired glucose metabolic activity in these patients correlated closely with the severity of preoperative neurological dysfunction [9]. Recent studies by another group demonstrated that spinal cord regional changes in ^{18}F-FDG uptake have prognostic significance in cervical myelopathy [10, 11]. Thus, it is possible that the combination of MRI and ^{18}F-FDG PET could uncover new features of cervical compressive myelopathy with respect to prognosis.

The present study was designed to evaluate the utility of three-dimensional (3D)-MRI/^{18}F-FDG PET fusion imaging in the detection of spinal cord lesions and define intramedullary signal changes on MRI and local glucose metabolic rate measured on ^{18}F-FDG PET in relation to clinical outcome and the prognosis.

29.1.1 MRI/^{18}F-FDG PET Image Fusion and Assessment

Our study included 24 patients with diagnosis of cervical compressive myelopathy (cervical spondylotic myelopathy: CSM 20 cases; ossification of posterior longitudinal ligament: OPLL 4 cases). Their neurological statuses were evaluated using the

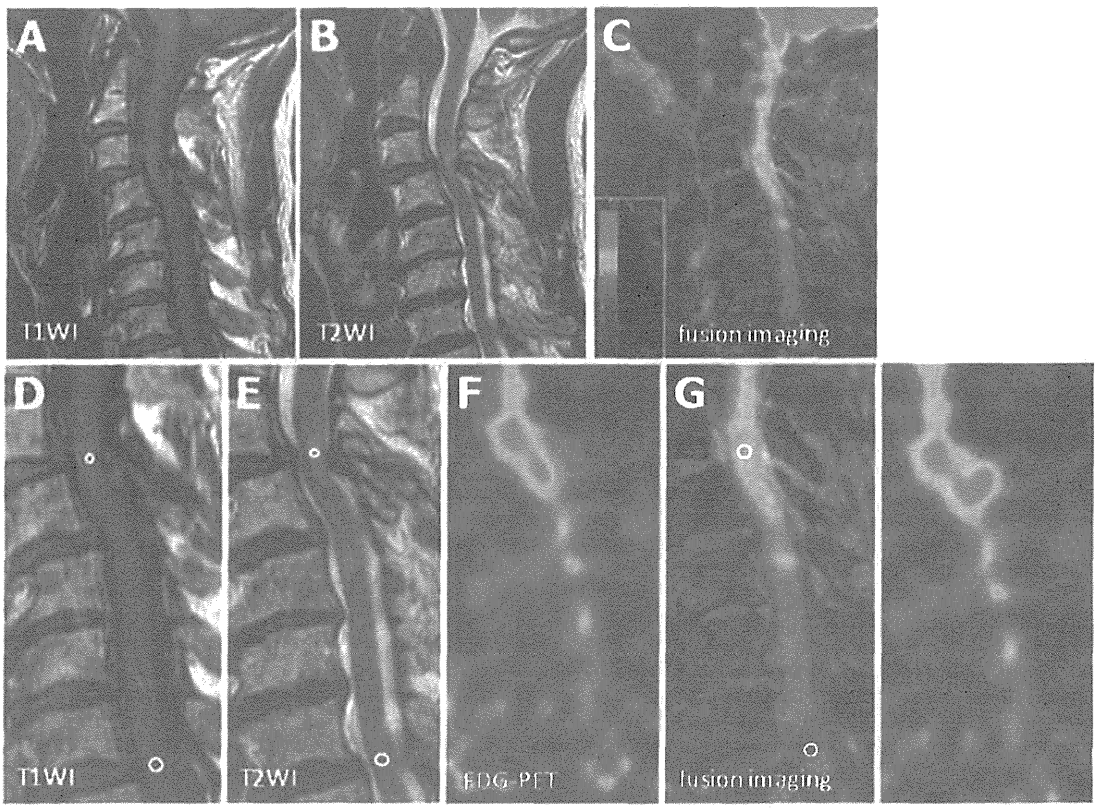

Fig. 29.1 An 80-year-old woman with cervical spondylotic myelopathy was treated surgically and showed a neurological improvement rate of 75.0 % at follow-up. (**a**) Midsagittal T1-weighted MRI, (**b**) midsagittal T2-weighted MRI, (**c**) MRI/PET fusion imaging (**d**, **e**), (**f**) ^{18}F-FDG PET sagittal image, and (**g**) MRI/PET fusion sagittal slice demonstrate a focal increase in ^{18}F-FDG uptake at the level of increased signal intensity lesion (Reprinted, with permission, from [29])

Japanese Orthopaedic Association (JOA) scoring system and the involved levels of compression were assessed using 3T MRI and ^{18}FDG-PET fusion imaging. Signal intensity change in the cord was qualitatively assessed on both T1- and T2-weighted images. In quantitative analysis of the signal change, the signal intensity ratio (SIR) on both T1-WIs and T2-WIs was calculated by the following equation:

$$SIR=\left[\frac{mid\text{–}sagittal\ cervical\ spinal\ cord\ on\ signal\ intensity\ at\ lesions\left(0.05\,cm^2\right)}{mid\text{–}sagittal\ normal\ cord\ signal\ intensity\ on\ the\ cervical\ disc\ levels\ between\ C7\ and\ T1\left(0.3\,cm^2\right)}\right]$$

Using the Advantage Workstation (GE Healthcare), the same slices of cervical 3D-MRI using 3.0 Tesla (T) Signa system and ^{18}F-FDG PET images were fused automatically. On fusion images, the maximal count at the lesion was adopted as the standardized uptake value (SUV_{max}). The SUV ratio, similar to SIR, (SUVR) was also calculated.

Examples are shown in Figs. 29.1 and 29.2. Figure 29.1 shows a significant increase in ^{18}F-FDG uptake (SUV_{max} =2.50, SUVR=1.84) at the level of the lesion

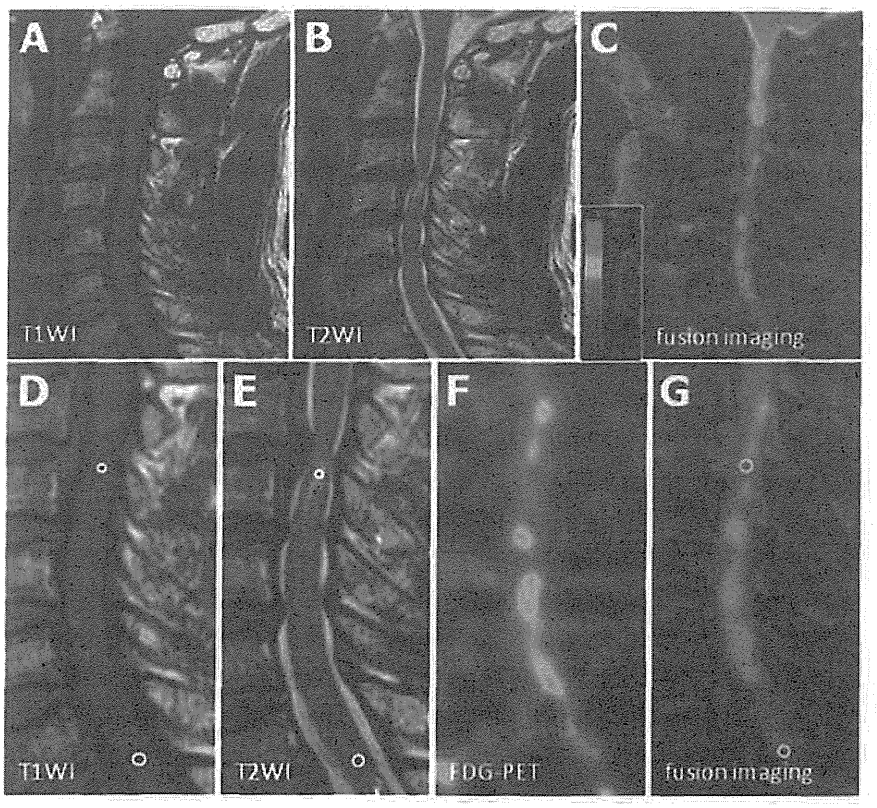

Fig. 29.2 A 62-year-old man with cervical spondylotic myelopathy was treated surgically and showed a poor neurological improvement rate of 28.6 % at follow-up. (**a**) Midsagittal T1-weighted MRI, (**b**) midsagittal T2-weighted MRI, (**c**) MRI/PET fusion imaging (**d**, **e**), (**f**) ^{18}F-FDG PET sagittal image, and (**g**) MRI/PET fusion sagittal slice demonstrate inconspicuous ^{18}F-FDG uptake at the level of lesion with increased signal intensity (Reprinted, with permission, from [29])

(SIR on T1-WI = 1.29, SIR on T2-WI = 1.55). The neurological improvement rate was considered good (75.0 %) at follow-up. On the other hand, Fig. 29.2 demonstrates the no increase in ^{18}F-FDG uptake (SUV_{max} = 1.60, SUVR = 0.87) at the level of the lesion (SIR on T1-WI = 0.99, SIR on T2-WI = 1.48). The neurological improvement rate at follow-up was poor (28.6 %).

29.1.2 Relationship Between Signal Intensity Ratio on MRI and Clinical Outcome

The SIR on T1-WIs correlated significantly with preoperative JOA score (R = 0.430; p < 0.05) and postoperative neurological improvement (R = 0.617; p < 0.01). However, there were no correlation between high change in intramedullary signal intensity on T2-WIs and preoperative JOA score (R = 0.174) or postoperative neurological improvement (R = 0.256).

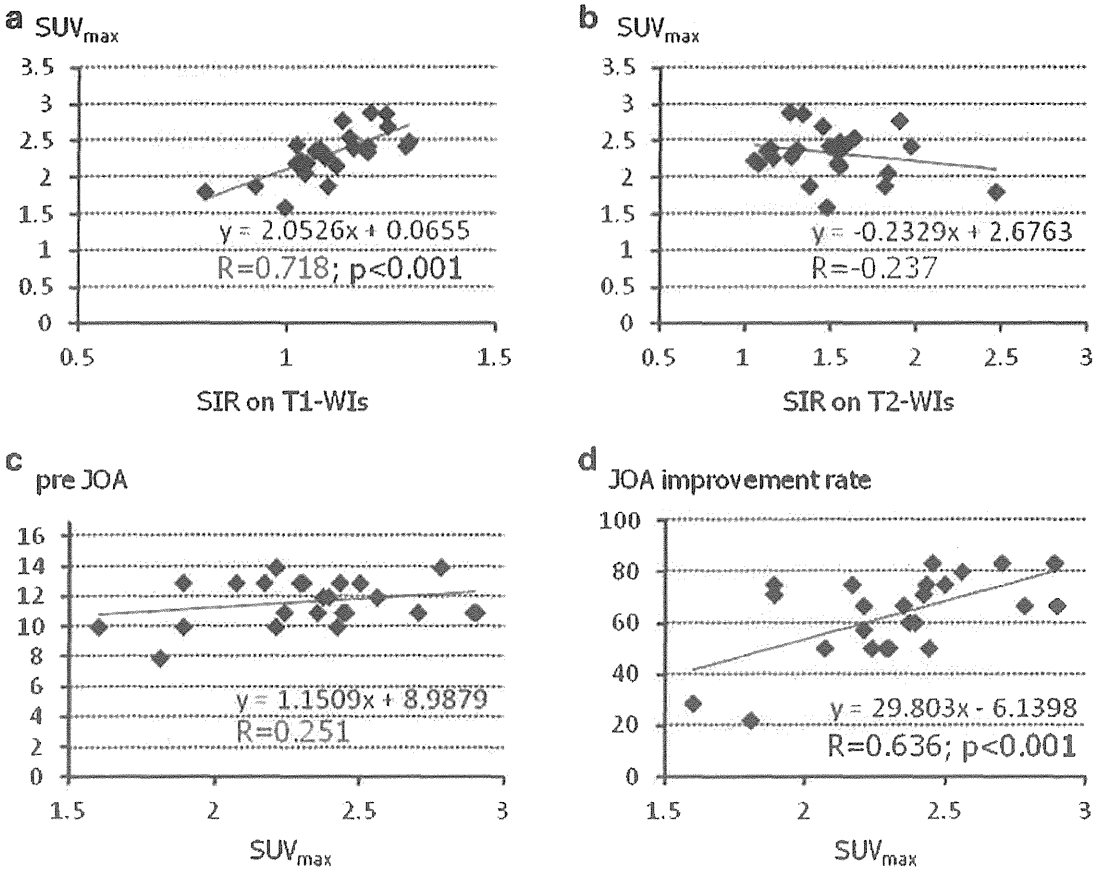

Fig. 29.3 Relationship between SUV measured at the lesion with increased signal intensity on MRI/PET fusion image and signal intensity ratio (SIR) and neurological scores. SUV_{max} at the sagittal lesion with increased cord intensity correlated strongly with the SIR on T1-WIs (**a**) but not on T2-WIs (**b**). SUV_{max} did not correlate with preoperative JOA score (**c**), but correlated with postoperative neurological improvement (**d**) (Reprinted, with permission, from [29])

29.1.3 Clinical Significance of SUV_{max} for Lesions with Increased Signal Intensity

Figure 29.3 shows the relationship between SUV_{max} for lesions with increased signal intensity on the sagittal plane and SIR on T1-WIs and T2-WIs as well as neurological scores. SUV_{max} for such lesions correlated significantly with SIR on T1-WIs (R=0.718; p<0.001, Fig. 29.3a) but not on T2-WIs (R=0.237, Fig. 29.3b). Furthermore, SUV_{max} correlated with postoperative neurological improvement (R=0.636; p<0.001, Fig. 29.3d) but not with preoperative JOA score (R=0.251, Fig. 29.3c).

29.1.4 Clinical Significance of the SUV Ratio

Figure 29.4 shows the relationship between SUVR and SIR on T1-WIs and T2-WIs as well as neurological score. SUVR correlated significantly with SIR on T1-WIs (R=0.704; p<0.001, Fig. 29.4a) but not on T2-WIs (R=0.210, Fig. 29.4b).

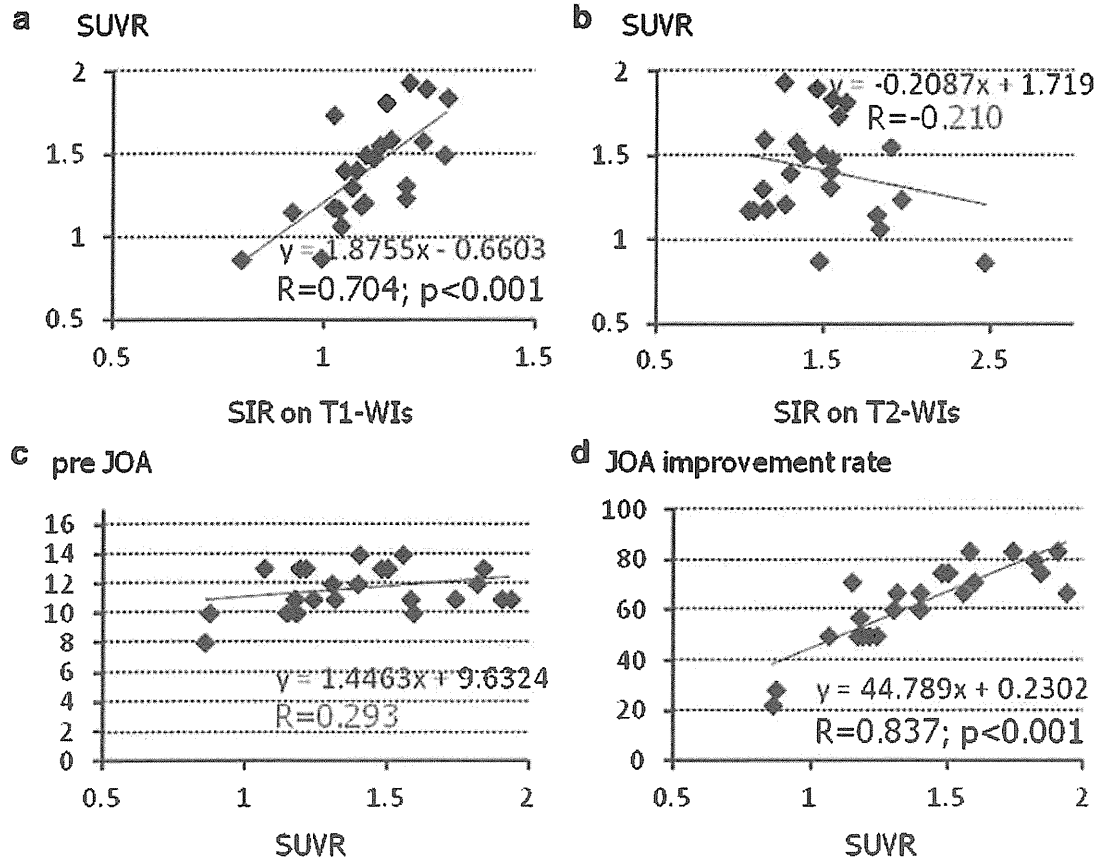

Fig. 29.4 Relationship between SUV ratio (SUVR) on MRI/PET fusion image and signal intensity ratio (SIR) and neurological scores. SUVR correlated strongly with SIR on T1-WIs (**a**) but not on T2-WIs (**b**). SUVR did not correlate with preoperative JOA score (**c**), but correlated with postoperative neurological improvement (**d**) (Reprinted, with permission, from [29])

Furthermore, SUV_{max} correlated significantly with postoperative neurological improvement, and the correlation coefficient was much higher than that of SUV_{max} for lesions with increased signal intensity on the sagittal plane ($R=0.837$; $p<0.001$, Fig. 29.4d), but not with preoperative JOA score ($R=0.293$, Fig. 29.4c).

29.2 Discussion

Elucidation of the factors that contribute to prognosis of patients with CSM and OPLL has been investigated by several groups [5, 12–15]. It is important to know those factors that determine neurological improvement after surgery. Age at surgery [16], duration of neurological symptoms [5, 13, 14, 16–18], and existence of signal changes on preoperative MRI [2–4, 19, 20] have been considered key predictors of surgical outcome. These factors could also have a significant impact on the surgical outcome of the patients in the present study as well, although we focused herein on the signal intensity changes on MRI and local glucose metabolism at the affected mono-segmental spinal cord lesion on PET using high-resolution MRI/PET fusion imaging.

While the MRI provides the highest specificity in the assessment of morphological changes and intramedullary state of the spinal cord, it is almost impossible to estimate the potential recovery of the spinal cord on preoperative MRI without quantitative analysis. Furthermore, the signal intensity on the MRI is irregular in each scan because different sequence parameters are set for each individual patient. On the other hand, ^{18}F-FDG PEt allows visualization of the metabolic activity of the spinal cord neural tissue in the same condition in each scan, and this parameter correlates closely with neurological prognosis. We quantified previously glucose utilization in the cervical spinal cord of patients with myelopathy [8]. Furthermore, Kamoto et al. [7] reported that the normal metabolic rate of glucose utilization in the cervical spinal cord (SUV) in healthy Japanese subjects (age, 40–70 years) was 1.93 ± 0.23, although this value was found to be 2.12 ± 0.48 and 1.84 ± 0.23 by Nakamoto et al. [21] and Floeth et al. [11], respectively. In another study, we reported that patients with mild to moderate myelopathy have significantly high SUV of the entire cervical spinal cord, while those with marked and profound tetraparesis had significantly low SUV [9]. Thus, a high SUV seems to reflect hyperactive neuronal activity within the spinal cord. In our latest study, patients with poor neurological improvement rate were found to have low preoperative SUV and significantly low postoperative neurological improvement [22]. Unfortunately, our results showed that preoperative SUV was not significantly different among patients with increased signal intensity on MRI.

The combination of the same slice 2 highest-end modalities (3D-MRI using 3T MRI and ^{18}F-FDG PET) in near real-time simultaneous scan has enabled us to image the metabolic function with detectable accuracy at the cervical spinal cord level. Our results showed that ^{18}F-FDG PET is more suitable and sensitive for the detection of changes in low-signal intensity on T1-weighted images on MRI/PET fusion imaging. Our results also suggested that SUV_{max} for lesions with increased signal intensity correlates with the SIR on T1-WIs and postoperative neurological outcome, but not with SIR on T2-WIs. Additionally, the SUVR is more sensitive to predict neurological improvement than SIR on T1-WIs or SUV_{max} in signal intensity lesions. Floeth et al. [10] demonstrated a significant decrease in ^{18}F-FDG uptake in the area of the lower cervical cord in patients with myelopathy than the control group. This could be the reason that made SUVR a more sensitive factor than SUV_{max} at the signal intensity lesion.

The present quantitative study based on MRI/PET fusion also showed no correlation with SIR on T2-WIs, while SIR on T1-WIs correlated with preoperative JOA score and postoperative neurological improvement. Theoretically, progressive changes should be observed as a high-signal intensity in the intramedullary lesion in patients with cervical compressive myelopathy. High-signal intensity is observed on T2-weighted MRI in patients with early-stage myelomalacia. Some patients at an intermediate stage display a variable degree of cystic necrosis of the central gray matter, which is better visualized on T2-weighted MRI. Finally, central cystic degeneration, syrinx formation, and atrophy are the main features of late-stage myelomalacia [23, 24]. On the other hand, the significance of decreased signal intensity on T1-weighted MRI has also been studied. Several groups have confirmed